QUARTERLY OF APPLIED MATHEMATICS
JANUARY 1985

ON STABILITY DIAGRAMS FOR DAMPED HILL EQUATIONS*

By

PAULI PEDERSEN

The Technical University of Denmark

Abstract. In previous works, the Galerkin approach is shown to be most efficient for quantitative stability analysis of the solutions to Hill equations. This approach, furthermore, should be recognized to be a theoretical tool as well, which enables us in a most simple way to prove a number of theorems on decoupling, symmetry and other similarities related to the stability diagrams.

In addition to the classification of solution functions we classify the possible excitation functions. Finally, a two parameter excitation function $\phi = \cos 2\tau + a_6 \cos 6\tau + a_{10} \cos 10\tau$, belonging to the class here termed as extended harmonic functions is discussed specifically, and detailed stability diagrams are presented. The accuracy of the analysis is verified.

1. Introduction. The stability analysis for the solutions to differential equations with periodic coefficients has been a challenge for more than one hundred years. In spite of the efforts the available quantitative results in terms of stability diagrams are rather meagre, also for the case of a single differential equation and even for the case of a harmonic periodic coefficient, here termed the excitation function. This should also be seen in the light of the fact that computers have been available for more than twenty years now. An approach suggested in [1] still seems to be advantageous compared with alternative approaches, and in this paper we shall extend the description and present new results, analytically as well as numerically.

Three alternative approaches are frequently used. The perturbation method is based on the assumption of small parameters, and seldom is the term "small" quantified. Often results are presented which far exceed the assumption made. The second approach is numerical integration over one period, using classical Floquet theory. The critical comment to this method is that it concentrates on specific parameters, and if more general stability diagrams have to be evaluated, it will be very computer-costly. Besides, numerical approximations are inherent in the determination. The third approach is based on Hill's infinite determinants. For a more detailed discussion of the three approaches, see Nayfeh & Mook [2].

---

*Received September 12, 1983.

The approach of [1], also used in the present paper, presents some similarities to the perturbation approach as well as to the approach with Hill's infinite determinants, but the negative aspects of these approaches are omitted, and the way of thinking is also quite different (being more engineering oriented). Furthermore, we are not satisfied with only knowing stability/instability boundaries.

To make this last point more clear let us assume a Hill equation with damping

$$y'' + 2c_0 y' + (a_0 + 2q_0\phi_0(\tau))y = 0, \tag{1.1}$$

where all quantities are real. The parameters are $c_0 \geqslant 0$ for damping, a_0 for excitation level, q_0 for excitation amplitude, and $\phi_0(\tau)$ is the π-period excitation function. With y' defined as $\partial y/\partial\tau$ our goal is to determine whether $y = y(\tau)$ is stable, i.e. we are not interested in the solution corresponding to specific initial conditions. On the other hand, we want quantitative information about the behaviour corresponding to specific data c_0, a_0, q_0, $\phi_0(\tau)$.

To do this we introduce *the free parameter* c which is not a physical damping but a complex quantity

$$c = \alpha + i\omega,\ i^2 = -1. \tag{1.2}$$

This parameter is introduced by the variable substitution

$$y(\tau) = e^{(c-c_0)\tau}z(\tau) = e^{(\alpha-c_0)\tau}e^{i\omega\tau}z(\tau), \tag{1.3}$$

and we get a new damped Hill equation

$$z'' + 2cz' + (a + 2q\phi(\tau))z = 0, \quad \text{with} \tag{1.4}$$

$$a = a_0 + c^2 - c_0^2 \Rightarrow a - c^2 = a_0 - c_0^2, \quad \text{and}$$

$$q\phi(\tau) = (q/A)(\phi(\tau)A) = q_0\phi_0(\tau) \Rightarrow q = q_0 A,\ \phi = \phi_0/A$$

where A is a normalization constant, described in Sec. 3.

If $c = 0$ this is the classical transformation from a damped Hill equation to an undamped Hill equation. However, as we shall see, dealing with c as well as c_0 enables the quantitative interpretation, and is a more direct approach than the classical formulation with characteristic exponent, although in principle, it is the same.

Now the eigenvalue problem that makes $z(\tau)$ a 2π-period solution is formulated, returning c as the eigenvalue when c_0, a_0, q_0, $\phi_0(\tau)$ is given. In general, we find

$$c = c(c_0, a_0, q_0, \phi_0(\tau)), \tag{1.5}$$

and prove that c is either pure real $c = \alpha$ or pure imaginary $c = i\omega$. By means of (1.3) the two cases give for $c^2 > 0$

$$y(\tau) = e^{(\alpha-c_0)\tau}z(\tau), \tag{1.6}$$

i.e. flutter (dynamic instability) for $\alpha > c_0$, 2π-period critical solutions for $\alpha = c_0$, and damped-periodic solutions for $\alpha < c_0$.

For $c^2 < 0$ we get

$$y(\tau) = e^{-c_0\tau}e^{i\omega\tau}z(\tau), \tag{1.7}$$

i.e. a solution which is a product of two limited periodic solutions, which are damped for $c_0 > 0$. We thus see how c gives the quantitative information on the behaviour independent of the specific initial conditions.

Often the Bubnov-Galerkin method is classified as a numerical technique and perturbation methods as analytical techniques. In the author's opinion this classification is misleading. By the Bubnov-Galerkin expansion we shall in this paper prove new valuable theorems in addition to those proved in [1]. We shall see also that the small parameter asymptotic expansions are easily evaluated from the Galerkin approach. Without losing the results from perturbation analysis, we thus have an approach, not depending on small parameters, which returns theoretical as well as numerical results.

In Sec. 2 we describe and classify the possible excitation functions. Then the solution functions are classified, and in Sec. 4 the approach of [1] is described shortly. Details with theorems and proofs are given in the appendix. In [1] the excitation function $\phi_0(\tau) = \cos 2\tau + a_4 \cos 4\tau$ is studied in detail, and in [3], the excitation function $\phi_0(\tau) = (1 + \varepsilon \cos 2\tau)^{-1}$ is studied by its Fourier transform. In this paper we shall concentrate on the detailed stability diagrams for $\phi_0(\tau) = \cos 2\tau + a_6 \cos 6\tau + a_{10} \cos 10\tau$, that is excitation functions belonging to the class here termed as extended harmonic functions.

2. Classification of excitation functions. The Hill equation, written in the standard form (1.1) assumes the excitation function ϕ_0 to be a π-period function, which we describe by

$$\phi_0(\tau) = \sum_{k=1,3,\dots} a_k \sin(k+1)\tau + \sum_{k=2,4,\dots} a_k \cos k\tau, \tag{2.1}$$

$$\text{assuming } a_1, a_2 \neq 0, 0.$$

Thus, the constants a_k are the parameters of the excitation function.

Important simplifications appear in the stability analysis, both when ϕ_0 is an even function and when it is an odd function. Furthermore, the results of the stability analysis are not influenced by the origo τ_0 of time, and some functions are even in relation to some origo, say $\cos 2\tau$ for $\tau_0 = 0$, and odd in relation to some other origo, say $\cos 2\tau$ for $\tau_0 = \pi/4$. As the simplifications for even functions are not the same as those for odd functions, we get a class of excitation functions with joint simplifications.

The nomenclature for the parameter a_0 in the standard form (1.1) should be seen in relation to the parameters a_k of the description (2.1). By this description the excitation function is normalized to

$$\int_0^{\pi} \phi_0(\tau)\, d\tau = \int_0^{\pi} \phi(\tau)\, d\tau = 0, \tag{2.2}$$

which holds independent of a_k in (2.1). To get a comparable effect of the parameter q in the standard form (1.4) we choose furthermore to normalize $\phi(\tau)$ by

$$\int_0^{\pi} \phi^2(\tau)\, d\tau = \pi/2, \tag{2.3}$$

which, by (2.1), gives the normalization constant A defined in (1.4) as

$$A^2 = \sum_{k=1,2,3,\dots} a_k^2. \tag{2.4}$$

The excitation functions are classified by the following four classes:

$$\phi(\tau) := \pi\text{-periodic satisfying (2.2) and (2.3), in general neither even nor odd for any origo } \tau_0. \tag{2.5}$$

$$\bar{\phi}(\tau) := \pi\text{-periodic satisfying (2.2) and (2.3), even for some origo } \bar{\tau}_0\text{, but not odd for any origo.} \tag{2.6}$$

$$\hat{\phi}(\tau) := \pi\text{-periodic satisfying (2.2) and (2.3), odd for some origo } \hat{\tau}_0\text{, but not even for any origo.} \tag{2.7}$$

$$\tilde{\phi}(\tau) := \pi\text{-periodic satisfying (2.2) and (2.3), even for some origo } \bar{\tau}_0\text{, and odd for some origo } \hat{\tau}_0. \tag{2.8}$$

This last class includes the harmonic functions and might be termed extended harmonic functions.

Examples related to the description (2.1) may be given as follows:

$$\phi(\tau) = (\sin 2\tau + \cos 2\tau + \sin 4\tau + \cos 4\tau)/\sqrt{4}\,, \tag{2.9}$$

$$\bar{\phi}(\tau) = (\cos 2\tau + \cos 4\tau)/\sqrt{2}\,, \tag{2.10}$$

$$\hat{\phi}(\tau) = (\sin 2\tau + \sin 4\tau)/\sqrt{2}\,, \tag{2.11}$$

$$\tilde{\phi}(\tau) = (\cos 2\tau + \cos 6\tau + \cos 10\tau)/\sqrt{3}\,, \tag{2.12}$$

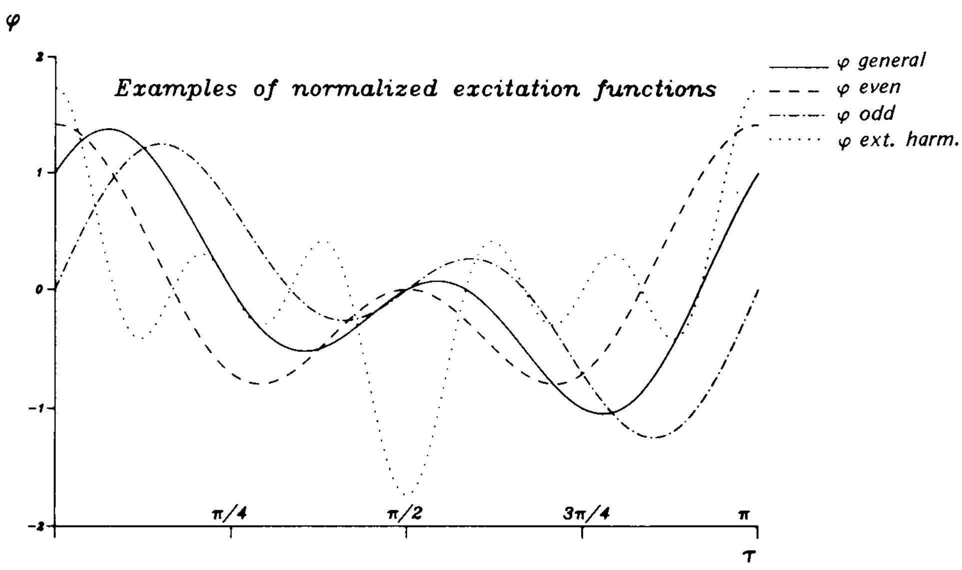

FIG. 2.1. Normalized excitation functions.

and these functions are shown in Fig. 2.1. From this figure we note some properties which may also be proved algebraically:

$$\begin{aligned}&\phi \text{ needs a full period for its description,}\\ &\bar{\phi} \text{ and } \hat{\phi} \text{ only need half a period for their description,}\\ &\tilde{\phi} \text{ only needs a quarter of a period for its description.}\end{aligned} \tag{2.13}$$

3. Classification of solution functions. The quantitative stability analysis of the solutions to Hill equations with damping is for given $\phi(\tau)$ reduced (cf. [1]) to the solution of an eigenvalue problem with the triple (c, q, a) as eigenvalue to

$$\begin{gathered} z'' + 2cz' + (a + 2q\phi(\tau))z = 0,\\ z(\tau) = z(\tau + 2\pi), \qquad z'(\tau) = z'(\tau + 2\pi). \end{gathered} \tag{3.1}$$

Note that π-periodic solution functions

$$z(\tau) = z(\tau + \pi), \qquad z'(\tau) = z'(\tau + \pi), \tag{3.2}$$

are included in this formulation.

This eigenvalue problem is then solved by the Bubnov-Galerkin procedure using the expansion

$$\begin{aligned} z(\tau) &= \sum_{n=1,2,\dots} b_n v_n(\tau),\\ v_1 &= 1,\\ v_n &= \cos\frac{n}{2}\tau, \qquad n = 2,4,\dots,\\ v_n &= \sin\frac{(n-1)}{2}\tau, \qquad n = 3,5,\dots. \end{aligned} \tag{3.3}$$

In this expansion we separate the π-periodic solution functions $z_1(\tau)$ from the remaining ones $z_2(\tau)$, i.e.

$$z(\tau) = z_1(\tau) + z_2(\tau) = \sum_{n=1,4,5,8,9,\dots} b_n v_n + \sum_{n=2,3,6,7,\dots} b_n v_n. \tag{3.4}$$

In relation to some simplified problems ($c = 0$ and $\phi = \bar{\phi}$, even functions) it is also practical to separate into even solution functions $\bar{z}(\tau)$ and odd solution functions $\hat{z}(\tau)$, i.e.

$$z(\tau) = \bar{z}(\tau) + \hat{z}(\tau) = \sum_{n=1,2,4,6,\dots} b_n v_n + \sum_{n=3,5,7,\dots} b_n v_n. \tag{3.5}$$

In total, the solution functions are then classified by the following four classes

$$\begin{aligned} \bar{z}_1(\tau) &:= \text{even } \pi\text{-periodic function}\\ &= \sum_{n=1,4,8,12,\dots} b_n v_n, \end{aligned} \tag{3.6}$$

$$\begin{aligned} \hat{z}_1(\tau) &:= \text{odd } \pi\text{-periodic function}\\ &= \sum_{n=5,9,13,\dots} b_n v_n, \end{aligned} \tag{3.7}$$

$$\begin{aligned}\bar{z}_2(\tau) &:= \text{even } 2\pi\text{-periodic (but not } \pi\text{-periodic) function} \\ &= \sum_{n=2,6,10,\dots} b_n v_n, \end{aligned} \tag{3.8}$$

$$\begin{aligned}\hat{z}_2(\tau) &:= \text{odd } 2\pi\text{-periodic (but not } \pi\text{-periodic) function} \\ &= \sum_{n=3,7,11,\dots} b_n v_n, \end{aligned} \tag{3.9}$$

and the arbitrary solution function $z(\tau)$ is added by

$$z(\tau) = \bar{z}_1(\tau) + \hat{z}_1(\tau) + \bar{z}_2(\tau) + \hat{z}_2(\tau). \tag{3.10}$$

4. Determinant factorizations. In this section we shall give a short presentation of the approach described in [1]. Details of the involved matrices, theorems and proofs are given in the appendix. The Bubnov-Galerkin expansion (3.3) results in a homogeneous set of equations for the constants b_n, contained in the vector $\{B\}$, i.e.

$$[S]\{B\} = \{0\}, \tag{4.1}$$

and thus the eigenvalue (c, q, a) of (3.1) is obtained by the determinant condition, which is worked out algebraically to a polynomial condition

$$|[S]| = \Delta(c, q, a) = 0. \tag{4.2}$$

To enable us study the influence of the excitation function, the parameters a_k in the description (2.1) are included and we get a more extended polynomial

$$\Delta(c, q, a, a_1, a_2, \dots) = 0. \tag{4.3}$$

Two important characteristics are proved to be valid for *all excitation functions*. Firstly, we proved the determinant to be independent of the sign of c, which we indicate by the squared parameter c^2

$$\Delta(c^2, q, a, a_k) = 0. \tag{4.4}$$

Secondly, the π-period solutions z_1 decouple from the remaining 2π-period solutions z_2 also for all ϕ, and this we write by the factorization

$$\Delta = \Delta_1 \Delta_2. \tag{4.5}$$

The remaining characteristics are only valid in relation to specific classes of excitation functions (2.6)–(2.8). For the class of *odd excitation functions* the determinant is independent of the sign of q, which we with (4.4) and (4.5) write

$$\Delta_1(c^2, q^2, a, a_k)\Delta_2(c^2, q^2, a, a_k) = 0. \tag{4.6}$$

This means that stability diagrams $a = a(q)$ for this class of excitation functions are symmetric with respect to the $q = 0$ line.

Simplicity in relation to the *even excitation functions* is only obtained when the damping parameter c is zero. When this is the case the even solution functions $\bar{z}$ decouple from the odd solution functions $\hat{z}$. Taking also (4.5) into consideration we get

$$\bar{\Delta}_1(q, a, a_k)\hat{\Delta}_1(q, a, a_k)\bar{\Delta}_2(q, a, a_k)\hat{\Delta}_2(q, a, a_k) = 0 \qquad (c = 0) \tag{4.7}$$

This means that a stability diagram (like the classical Strutt-Haines diagram) may be obtained with determinants of relatively low order, at the cost of dealing with four determinants.

The joint simplifications of (4.6) and (4.7) are then valid for the class (2.8) of *extended harmonic excitation functions*. Furthermore, it is proved in the appendix that $\bar{\Delta}_2(q,\dots) = \hat{\Delta}_2(-q,\dots)$ for this class, and we may therefore write

$$\bar{\Delta}_2(\pm q, a, a_k)\bar{\Delta}_1(q^2, a, a_k)\hat{\Delta}_1(q^2, a, a_k) = 0, \tag{4.8}$$

for this important class of excitation functions.

5. Stability diagrams for extended harmonic excitations. The class of extended harmonic excitation functions as defined by (2.8) may be described by a pure sine series: $a_1 = 1$ and then $a_k \neq 0$ only for $k = 5, 9, 13, \dots$, or by a pure cosine series $a_2 = 1$ and then $a_k \neq 0$ only for $k = 6, 10, 14, \dots$. Here, we choose the cosine description

$$\tilde{\phi}_0(\tau) = \cos 2\tau + \sum_{k=6,10,14,\dots} a_k \cos k\tau. \tag{5.1}$$

With no damping parameter ($c = 0$) the eigenvalue analysis according to (4.8) give rise to the three (four) separated determinant polynomials

$$\bar{\Delta}_1(q^2, a, a_6, a_{10}, \dots) = 0, \tag{5.2}$$

for the even π-period solution functions,

$$\hat{\Delta}_1(q^2, a, a_6, a_{10}, \dots) = 0, \tag{5.3}$$

for the odd π-period solution functions,

$$\bar{\Delta}_2(q, a, a_6, a_{10}, \dots) = \hat{\Delta}_2(-q, a, a_6, a_{10}, \dots) = 0, \tag{5.4}$$

for the even and odd remaining 2π-period solution functions.

To point out that our analysis also contains the results obtained by perturbation analysis, we shall focus primarily on the low order approximations for the 2π-period solutions. From the appendix (A.8) we read directly for $\underline{n = 1}$ with $a_2 = 1$:

$$a - 1 \pm q = 0 \Rightarrow a = 1 \mp q, \tag{5.5}$$

i.e. only information related to the main domain of instability. For the part $\underline{n = 1, 2}$ the second order determinants return

$$a^2 + (\pm q(1 + a_6) - 10)a + \left(q^2(-1 + a_6) \pm q(-9 - a_6) + 9\right) = 0, \tag{5.6}$$

which we solve approximately for $a_6 = 0$ as

$$\begin{aligned} a &\approx 1 \mp q - \frac{1}{8}q^2 \pm \frac{1}{64}q^3, \\ a &\approx 9 + \frac{1}{8}q^2 \mp \frac{1}{64}q^3. \end{aligned} \tag{5.7}$$

Note that not until $n = 1, 2$ is the second coefficient a_6 of the excitation function involved. Furthermore, we now also get information about the next (2π-period) domain of instability. For the part $\underline{n = 1, 2, 3}$, a_{10} also is involved, and we get information about three domains. Here we shall only give the resulting approximations for $a_6 = a_{10} = 0$, which give $a = a(q)$ explicitly

$$\begin{aligned} a &\approx 1 \mp q - \frac{1}{8}q^2 \pm \frac{1}{64}q^3, \\ a &\approx 9 + \frac{1}{16}q^2 \mp \frac{1}{64}q^3, \end{aligned} \tag{5.8}$$

and continuing for the part $\underline{n = 1, 2, 3, 4}$ we again get

$$\begin{aligned} a &\approx 1 \mp q - \frac{1}{8}q^2 \pm \frac{1}{64}q^3, \\ a &\approx 9 + \frac{1}{16}q^2 \mp \frac{1}{64}q^3. \end{aligned} \tag{5.9}$$

The intention of showing the explicit results (5.5), (5.7)–(5.9) is primarily to prove that these are also available with the present approach. In the author's opinion it is, however, more advantageous to *stay by the implicit results* like (5.6).

In the remaining part of the paper we shall concentrate on presenting stability diagrams for excitation functions (5.1), which are needed from the more practical point of view. The symbolic computer language of FORMAC [4], [5] is used to obtain higher order determinants analytically, and we write the resulting expression for the determinant

$$\Delta = \sum P_{ijklm} a^i q^j a_6^k a_{10}^l (c^2)^m = 0 \tag{5.10}$$

$(i, j, k, l, m$ non-negative integers$)$.

The resulting solutions to the five parameter polynomial (5.10) may then be presented in different forms, all of which are obtained by Newton-Raphson solutions to (5.10), which is very convenient because derivatives $\partial\Delta/\partial a$, $\partial\Delta/\partial q$, $\partial\Delta/\partial a_6$, $\partial\Delta/\partial a_{10}$ or $\partial\Delta/\partial(c^2)$ are easily obtained. Alternative forms are presented in [1], but here we restrict the presentation to diagrams which are specific related to a given normalized excitation function $\tilde{\phi}(\tau)$. The abcissa is $(a - c^2) = (a_0 - c_0^2)$ and the ordinate is $|q| = |q_0|A$. Thus in these diagrams we read directly the value of $c = \alpha + i\omega$ corresponding to specific data c_0, a_0, q_0, $\phi_0(\tau)$, and obtain from eq. (1.3) the quantitative information about stability.

6. Examples and practical aspects. Fig. 6.1 shows and numbers as 1–8 some specific excitation functions for which stability diagrams will be presented.

First, we want to see the influence of the "shape" of excitation and therefore show four joint diagrams in Figs. 6.2 and 6.3. These diagrams with results only for $c = 0$ (stability/instability boundaries with no damping, i.e. with $c_0 = 0$), are based on the fully factorized determinants (5.2)–(5.4), which makes high order expansions (high accuracy) possible. With reference to expansion (3.3), $n_{\max}$ for these results is 25, and we show the diagrams up to $|q| = 8$. Note the "coexistent" solutions (crossing curves) in the third domain of instability for excitation functions with $a_6 < 0$, i.e. for excitation functions 2, 7 and 8.

Now, in Figs. 6.2 and 6.3 we have pointed out the specific domain of $-2 \leqslant a \leqslant 6$, $0 \leqslant |q| \leqslant 2$ for which detailed stability diagrams are going to be presented. We see that in

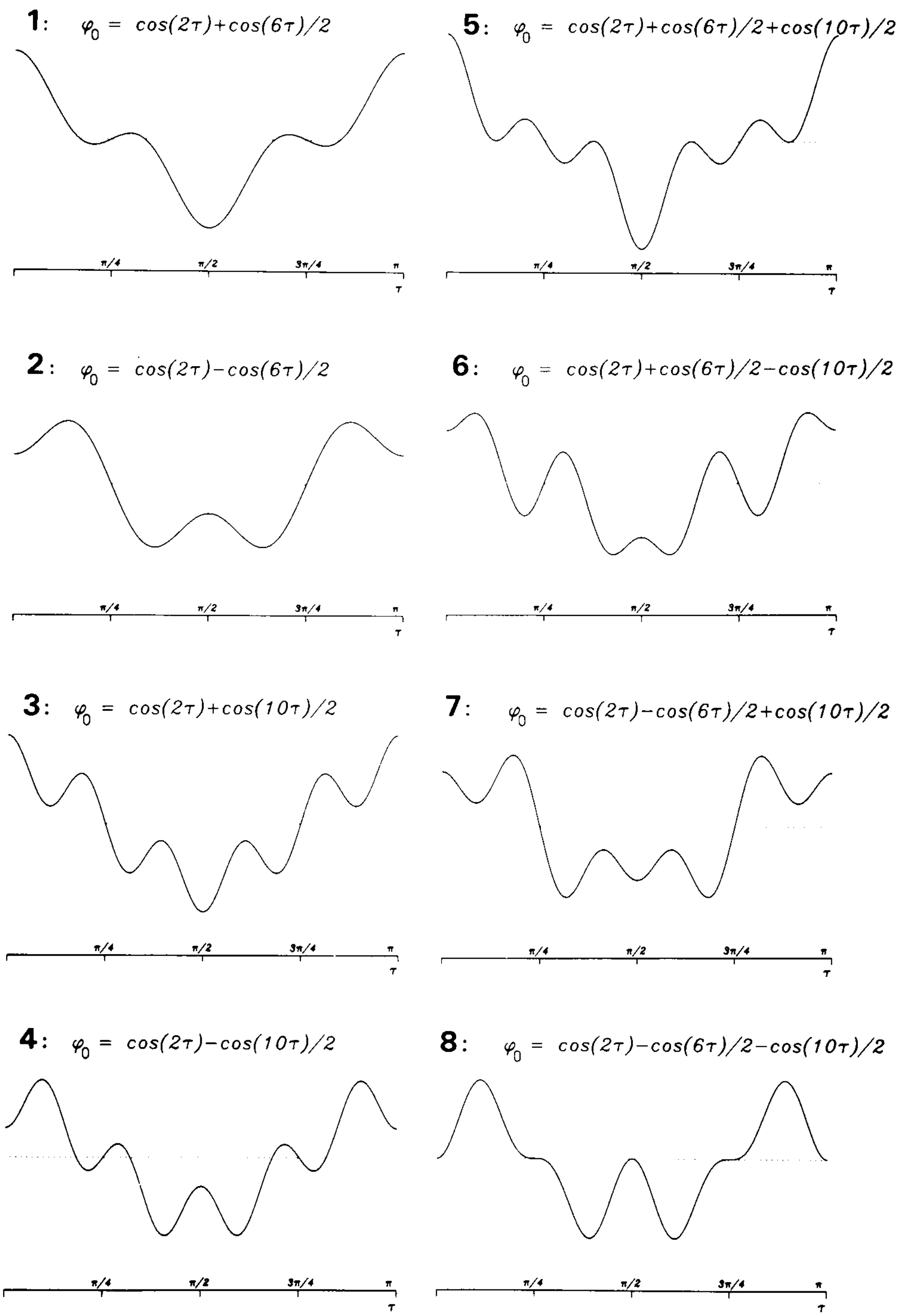

FIG. 6.1. "Shape" of the eight excitation functions for which stability diagrams are presented.

this domain the results are almost independent of the sign for the parameter a_{10} ($3 = 4$, $5 = 6$, $7 = 8$). Thus we only present results corresponding to the excitation functions 1, 2, 3, 5 and 7.

The detailed stability diagrams of Figs. 6.4–6.8 have a common symbolism. Full lines are identical to the results in Figs. 6.2, 6.3, and are thus high accuracy results corresponding to $c = 0$. Dashed lines correspond to $c^2 < 0$, i.e. $\alpha = 0$, $\omega = \pm\sqrt{-c^2}$, and the domains with these lines are always stable according to Eq. (1.7). The dash-dot lines correspond to $c^2 > 0$, i.e. $\alpha = \sqrt{c^2}$, $\omega = 0$, and the domains with these lines are stable/unstable depending on the actual c_0 according to Eq. (1.6).

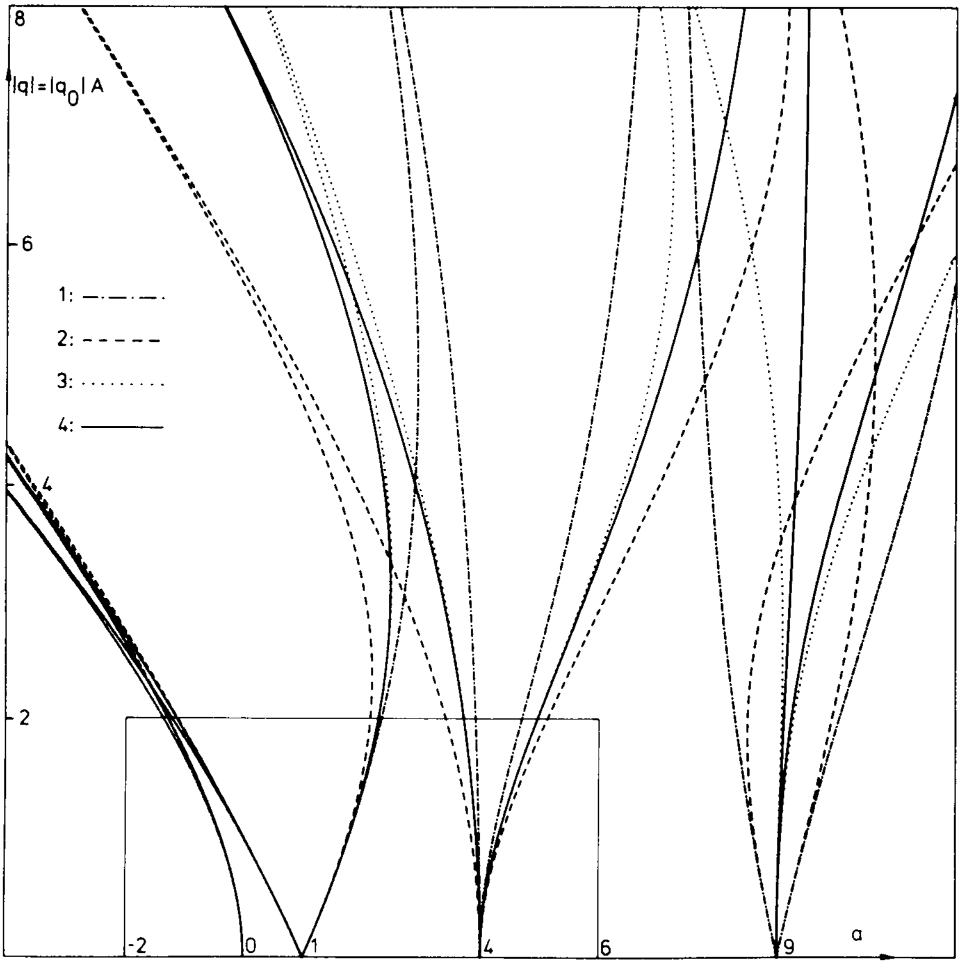

FIG. 6.2. Non-detailed but extended stability diagrams for excitation functions 1–4 as defined in Fig. 6.1.

A few comments on the practical aspects of obtaining the lines, i.e. about the Newton-Raphson solutions to (5.10):

As the solutions are non-unique, a good starting point is necessary, and thus the analytical solutions to $q = 0$ are used. From (1.4) with $q = 0$ and $z = e^{in\tau}$ $(n = 0, 1, \ldots)$ we get

$$\left(-n^2 + i2cn + a_0 + c^2 - c_0^2\right) = 0, \tag{6.1}$$

which gives

$$a_0 - c_0^2 = \left(n + \sqrt{-c^2}\right)^2, \tag{6.2}$$

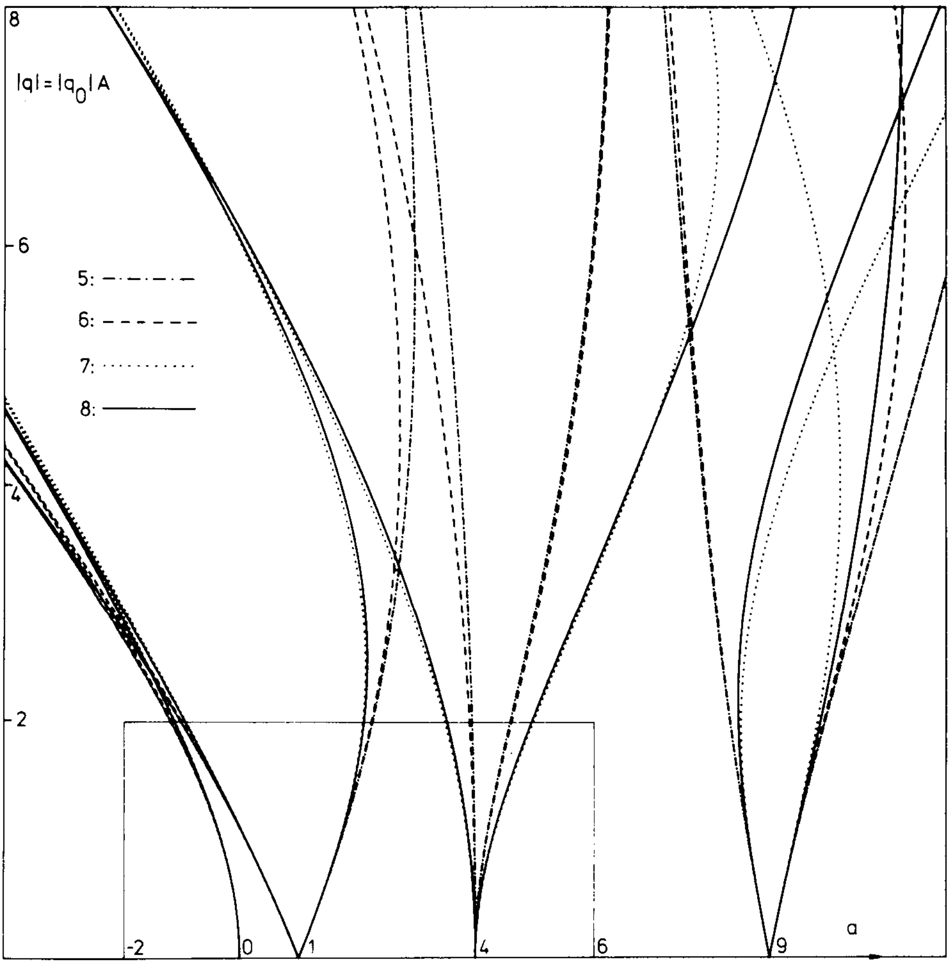

FIG. 6.3. Non-detailed but extended stability diagrams for excitation functions 5–8 as defined in Fig. 6.1.

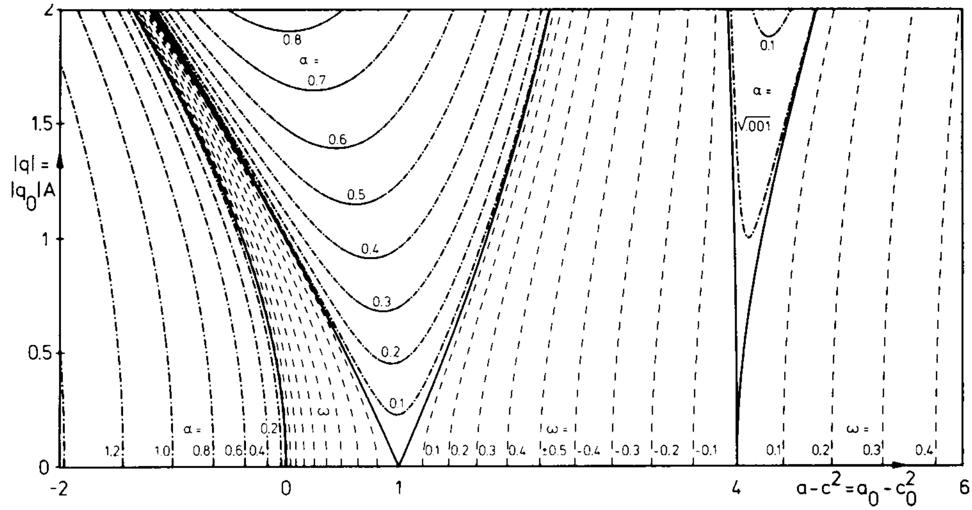

FIG. 6.4. Detailed stability diagram for

$$z'' + 2c_0 y' + \left(a_0 + 2q_0\left(\cos 2\tau + \frac{1}{2}\cos 6\tau\right)\right) y = 0.$$

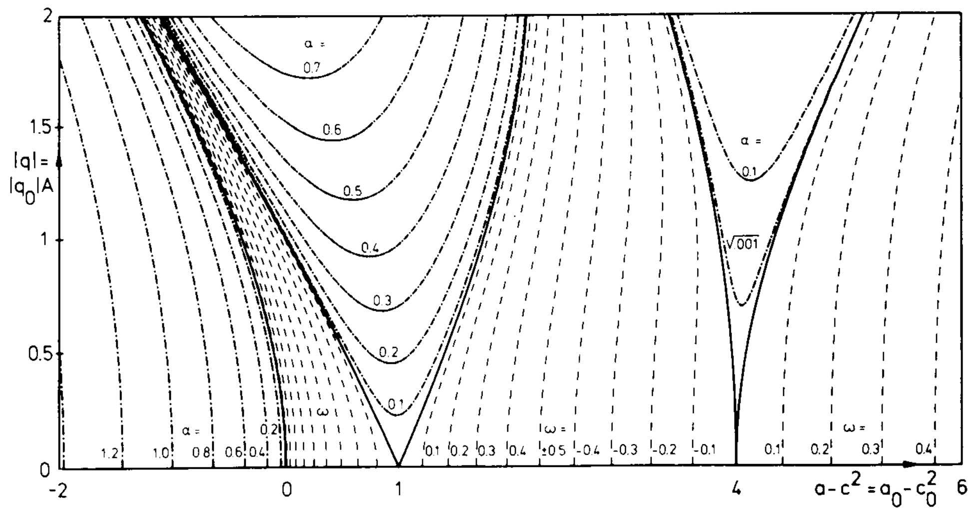

FIG. 6.5. Detailed stability diagram for

$$z'' + 2c_0 y' + \left(a_0 + 2q_0\left(\cos 2\tau - \frac{1}{2}\cos 6\tau\right)\right) y = 0.$$

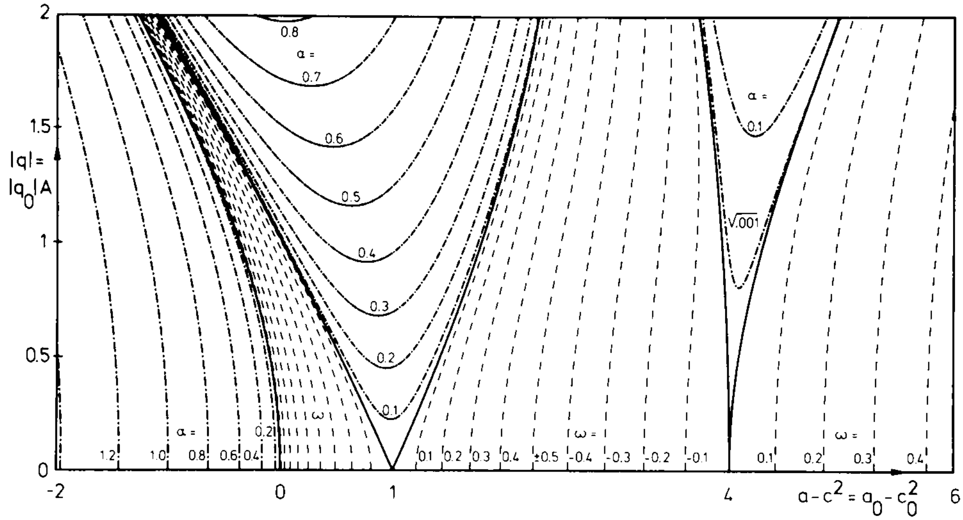

FIG. 6.6. Detailed stability diagram for

$$y'' + 2c_0y' + \left(a_0 + 2q_0\left(\cos 2\tau + \frac{1}{2}\cos 10\tau\right)\right)y = 0.$$

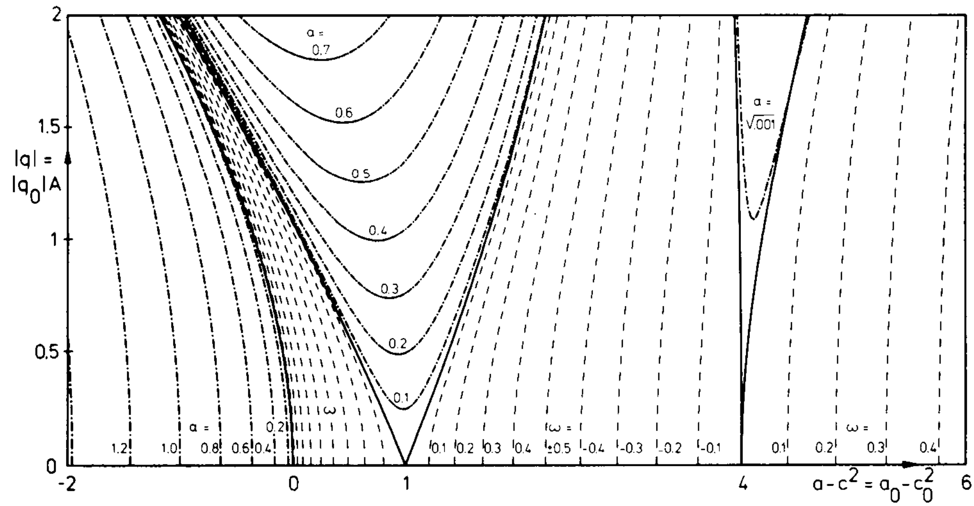

FIG. 6.7. Detailed stability diagram for

$$y'' + 2c_0y' + \left(a_0 + 2q_0\left(\cos 2\tau + \frac{1}{2}\cos 6\tau + \frac{1}{2}\cos 10\tau\right)\right)y = 0.$$

with $c^2 < 0$ for $n = 0$ and $c^2 > 0$ for $n = 1, 2, \ldots$. The curves starting from $q = 0$ are obtained as $a = a(q_0)$ for given c and then plotted as $q = q(a - c^2) = q(a_0 - c_0^2)$. The curves not reaching $q = 0$ are mostly obtained as $q_0 = q_0(a)$ and then plotted as $q = q(a - c^2)$. The reason for choosing $(a - c^2)$ as the abscissa will be shown later.

In the stability diagrams (Figs. 6.4–6.8) the accuracy of the dashed and dash-dotted lines correspond to $n_{\max}$ in expansion (3.3) equal to 13. The nice agreement with the high accuracy full lines shows that this is enough for the actual domain. The independent polynomials from Δ_1, and Δ_2, respectively, may also be mutually tested. As an example in the stable domain around $1 \lessapprox a \lessapprox 4$, we get from Eq. (1.7)

$$y_1 = e^{-c_0\tau} e^{i\omega_1\tau} e^{i1\tau} = y_2 = e^{-c_0\tau} e^{i\omega_2\tau} e^{i2\tau} \qquad \text{for } \omega_2 = \omega_1 - 1. \tag{6.3}$$

Test in agreement with this also return high accuracy.

Finally, tests are carried out in relation to simulated solutions with specific initial conditions. The CSMP [6] program is used for this and the results of nine simulations are shown in Fig. 6.9. This also gives an opportunity of showing how the stability diagrams are used to predict these results without carrying out the simulations.

Let our specific Hill equation be

$$y'' + 2c_0 y + \left(a_0 + 0.6(\cos 2\tau - 0.5\cos 6\tau + 0.5\cos 10\tau)\right) y = 0 \tag{6.4}$$

and we want to know the behavior $y = y(\tau)$ for the c_0, a_0 values listed in Table 6.1. In this table we have also determined the normalized q value corresponding to Eq. (6.4), and listed the α, ω values as read directly from stability diagram, Fig. 6.8.

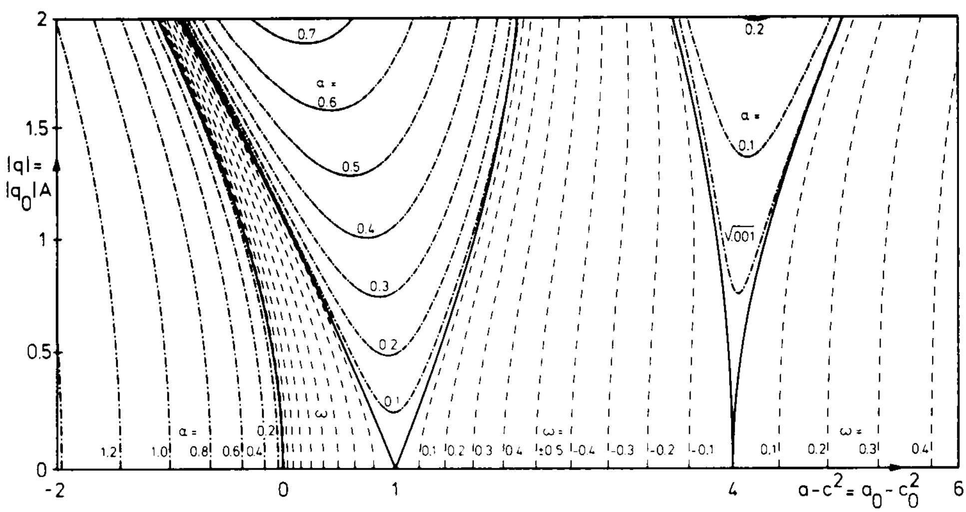

FIG. 6.8. Detailed stability diagram for

$$y'' + 2c_0 y' + \left(a_0 + 2q_0\left(\cos 2\tau - \frac{1}{2}\cos 6\tau + \frac{1}{2}\cos 10\tau\right)\right) y = 0.$$

Unstable solutions with high damping $c_0 = 0.1$.

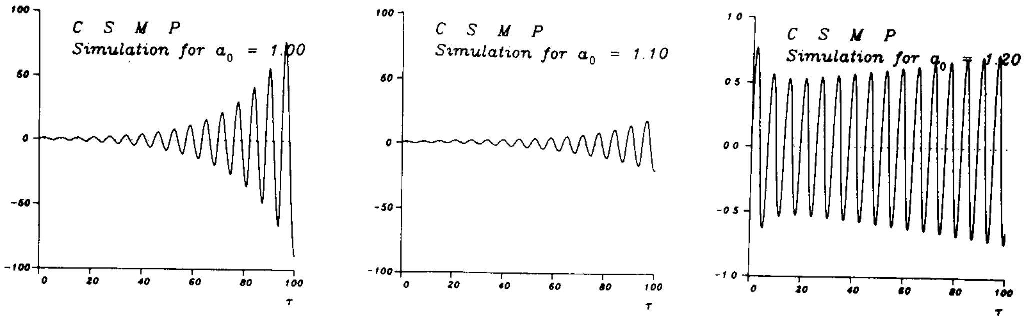

Stable solutions with high damping $c_0 = 0.1$.

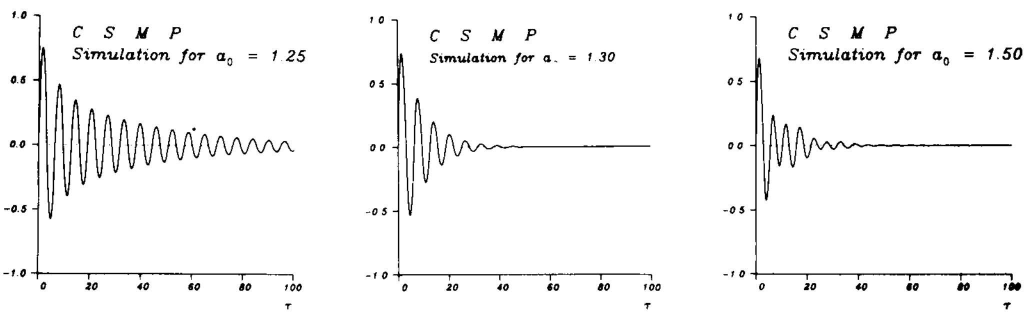

Stable solutions with weak damping $c_0 = 0.001$.

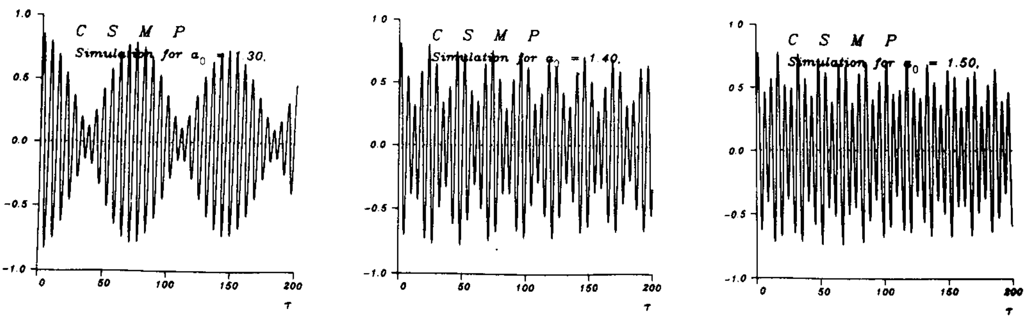

FIG. 6.9. CSMP [6] simulated solutions to eq. (6.4) based on the initial conditions $y(\tau = 0) = 0$ and $\partial y/\partial\tau(\tau = 0) = 1$.

$q_0 = 0.3, A^2 = 3/2, \Rightarrow q = q_0 A = 0.37$									
ϕ_0 as by stability diagram in Fig. 6.8									
c_0	0.1	0.1	0.1	0.1	0.1	0.1	0.001	0.001	0.001
a_0	1.0	1.1	1.2	1.25	1.3	1.5	1.3	1.4	1.5
$a_0 - c_0^2$	0.99	1.09	1.19	1.24	1.29	1.49	1.30	1.40	1.50
α	0.15	0.13	0.10	0.05	0	0	0	0	0
ω	0	0	0	0	0.01	0.18	0.02	0.13	0.19

TABLE 6.1. List of given parameters q_0, A, ϕ_0, c_0, a_0 for Eq. (6.4), and the corresponding stability parameters α, ω as interpolated from Fig. 6.8.

The first row of unstable solutions (in Fig. 6.9) and the first stable solution in the second row are directly seen to agree with the α values of Table 6.1. The highly damped solutions for $c_0 = 0.1$ in the second row make it difficult to see the influence of $\omega = 0.01$ and 0.18, respectively. However, in the last row with weak damping, $c_0 = 0.001$, the values of $\omega = 0.02$, 0.13 and 0.19 are directly seen to agree with the CSMP simulations.

We see that even for a damped Hill equation ($c_0 \neq 0$) the stability diagrams give directly quantitative information about the behaviour, and not only the classification stable/unstable.

7. Conclusions. Stability diagrams for Hill equations are effectively established by the approach based on a Galerkin expansion. This, in fact, is a natural choice because each "point" in the diagram constitutes an eigenvalue problem.

In the present paper we have primarily focused on the theoretical information on decoupling, symmetry, etc. that can be obtained from the appearance of the Galerkin coefficient matrix. Most of the theorems given in the appendix are well known, but it is interesting to note how easily they are obtained from the theory of determinants.

Joint simplifications are actual for a class of excitation functions termed "extended harmonics". All the numerical results are concentrated on a two-parameter function $\phi = \cos 2\tau + a_6 \cos 6\tau + a_{10} \cos 10\tau$ belonging to this class. Such excitation functions do not seem to have been studied before. Main results are the location of coexistent solutions in the third domain of instability for $a_6 < 0$ and, for moderate values of excitation, a rather weak dependence on the sign of a_{10}.

The detailed stability diagrams of the present paper are refined in a way, which make them directly useable also for damped Hill equations. The normalization of excitation functions and the choice of the abscissa to be $(a - c^2)$ and not just (a) add highly to the usefulness of the diagrams.

Appendix: Coefficient matrix of the Bubnov-Galerkin expansion with theorems of decoupling, symmetry and other similarities. Firstly, the total coefficient matrix is separated according to the separation z_1, z_2, defined in section three:

$$[S] = \begin{bmatrix} [S]_1, & [0] \\ [0], & [S]_2 \end{bmatrix}. \tag{A.1}$$

The two submatrices are individually separated according to the separations $\bar{z}$ and $\hat{z}$

$$[S]_1 = \begin{bmatrix} [S]_{\bar{1},\bar{1}}, & [S]_{\bar{1},\hat{1}} \\ [S]_{\hat{1},\bar{1}}, & [S]_{\hat{1},\hat{1}} \end{bmatrix}, \tag{A.2}$$

$$[S]_2 = \begin{bmatrix} [S]_{\bar{2},\bar{2}}, & [S]_{\bar{2},\hat{2}} \\ [S]_{\hat{2},\bar{2}}, & [S]_{\hat{2},\hat{2}} \end{bmatrix}, \tag{A.3}$$

and the eight submatrices are then listed, reordered but directly taken from [1]

$$[S]_{\bar{1},\bar{1}} = \tag{A.4}$$

$$\begin{bmatrix} 2a, & & & \\ & a-4, & & \\ & & a-16, & \\ & & & a-36 \\ \text{diagonal} & & & \end{bmatrix} + q \begin{bmatrix} 0, 2a_2, & 2a_4, & 2a_6, \\ & a_4, a_2+a_6, & a_4+a_8, \\ & & a_8, & a_2+a_{10}, \\ & & & a_{12}, \\ \text{symmetric} & & & \end{bmatrix}$$

$$[S]_{\hat{1},\hat{1}} = \tag{A.5}$$

$$\begin{bmatrix} a-4, & & \\ & a-16, & \\ & & a-36 \\ \text{diagonal} & & \end{bmatrix} + q \begin{bmatrix} -a_4, & a_2-a_6, & a_4-a_8, \\ & -a_8, & a_2-a_{10}, \\ & & -a_{12}, \\ \text{symmetric} & & \end{bmatrix}$$

$$[S]_{\bar{1},\hat{1}} = \tag{A.6}$$

$$c \begin{bmatrix} 0, & & \\ 4, 0, & & \\ & 8, 0, & \\ & & 12, 0 \\ \text{codiagonal} & & \end{bmatrix} + q \begin{bmatrix} 2a_1, & 2a_3, & 2a_5, \\ a_3, & a_1+a_5, & a_3+a_7, \\ -a_1+a_5, & a_7, & a_1+a_9, \\ -a_3+a_7, & -a_1+a_9, & a_{11}, \end{bmatrix}$$

$$[S]_{\hat{1},\bar{1}} = \tag{A.7}$$

$$-c \begin{bmatrix} 0, 4, & & \\ & 0, 8, & \\ & & 0, 12 \\ \text{codiagonal} & & \end{bmatrix} + q \begin{bmatrix} 2a_1, & a_3, & -a_1+a_5, & -a_3+a_7, \\ 2a_3, & a_1+a_5, & a_7, & -a_1+a_9, \\ 2a_5, & a_3+a_7, & a_1+a_9, & a_{11}, \end{bmatrix}$$

$$\begin{array}{ccccc} [S]_{\bar{2},\bar{2}} & = & [S]_{\hat{2},\hat{2}} & = \\ \text{(upper sign)} & & \text{(lower sign)} & \end{array} \tag{A.8}$$

$$\begin{bmatrix} a-1, & & \\ & a-9, & \\ & & a-25 \\ \text{diagonal} & & \end{bmatrix} + q \begin{bmatrix} \pm a_2, & a_2 \pm a_4, & a_4 \pm a_6, & a_6 \pm a_8, \\ & \pm a_6, & a_2 \pm a_8, & a_4 \pm a_{10}, \\ & & \pm a_{10}, & a_2 \pm a_{12}, \\ \text{symmetric} & & & \end{bmatrix}$$

$$
\begin{array}{cc}
[S]_{\bar{2},\hat{2}} \quad = & [S]^{T}_{\hat{2},\bar{2}} \quad = \\
\text{(upper sign)} & \text{(lower sign)}
\end{array}
\tag{A.9}
$$

$$
\pm c \left[\begin{array}{llll} 2, & & & \\ & 6, & & \\ & & 10, & \\ \text{diagonal} & & & \end{array}\right.
\qquad
+ q \left[\begin{array}{cccc}
a_1, & \pm a_1 + a_3, & \pm a_3 + a_5, & \pm a_5 + a_7, \\
a_1 + a_3, & a_5, & \pm a_1 + a_7, & \pm a_3 + a_9, \\
a_3 + a_5, & a_1 + a_7, & a_9, & \pm a_1 + a_{11},
\end{array}\right.
$$

THEOREM 1. The total determinant is equal to the product of the determinant of the π-period solutions and the determinant of the remaining 2π-period solutions, i.e. $\Delta = \Delta_1 \cdot \Delta_2$.

Proof. This follows directly from (A.1), which shows that the z_1 solutions decouple from the z_2 solutions.

THEOREM 2. The determinants Δ_1 and Δ_2 are both independent of the sign of c, i.e. $\Delta_1 = \Delta_1(c^2, \ldots)$ and $\Delta_2 = \Delta_2(c^2, \ldots)$.

Proof. The matrices $[S]_1$ and $[S]_2$ are both antimetric depending on c as seen from (A.6), (A.7) and (A.9). The determinant of a matrix is equal to the determinant of the transposed matrix, thus by the antimetric nature proving the independence of the sign of c.

THEOREM 3. The parameter $c = \alpha + i\omega$ is either pure real $c = \alpha$ or pure imaginary $c = i\omega$.

Proof. This follows directly from theorem 2, when c^2 is a real quantity.

THEOREM 4. For an odd excitation function $\hat{\phi}(\tau + \hat{\tau}_0) = -\hat{\phi}(-\tau + \hat{\tau}_0)$ the determinants Δ_1 and Δ_2 are both independent of the sign of q, i.e. $\Delta_1 = \Delta_1(q^2, \ldots)$ and $\Delta_2 = \Delta_2(q^2, \ldots)$. Stated in other terms: The resulting stability diagrams will be symmetric relative to the line $q = 0$.

Proof. A proof directly from Hill's equation is given in [1]. An alternative proof follows from the determinants calculated by

$$\Delta_1 = \left|[S]_{\bar{1},\bar{1}}\right| \left|[S]_{\hat{1},\hat{1}} - [S]_{\hat{1},\bar{1}}[S]^{-1}_{\bar{1},\bar{1}}[S]_{\bar{1},\hat{1}}\right|$$

$$\Delta_2 = \left|[S]_{\bar{2},\bar{2}}\right| \left|[S]_{\hat{2},\hat{2}} - [S]_{\hat{2},\bar{2}}[S]^{-1}_{\bar{2},\bar{2}}[S]_{\bar{2},\hat{2}}\right|$$

which is possible according to Gantmacher [7], p. 46. When $\hat{\phi}$ is described by a pure sine series, all $a_k = 0$ for k even, and then $[S]_{\bar{1},\bar{1}}$, $[S]_{\hat{1},\hat{1}}$, $[S]_{\bar{2},\bar{2}}$, $[S]_{\hat{2},\hat{2}}$ are all diagonal matrices independent of q, as seen from (A.4), (A.5) and (A.8). The independence of the sign of q then follows when the matrix multiplications are performed.

THEOREM 5. For an even excitation function $\bar{\phi}(\tau + \bar{\tau}_0) = \bar{\phi}(-\tau + \bar{\tau}_0)$ the determinants Δ_1, Δ_2 corresponding to no damping ($c = 0$) are equal to the product of the determinants of even solutions and the determinants of odd solutions, i.e. $\Delta_1 = \bar{\Delta}_1\hat{\Delta}_1$ and $\Delta_2 = \bar{\Delta}_2\hat{\Delta}_2$.

Proof. When $\bar{\phi}$ is described by a pure cosine series, all $a_k = 0$ for k odd and then for $c = 0$ we have by (A.6), (A.7) and (A.9) that $[S]_{\bar{1},\hat{1}} = [S]_{\hat{1},\bar{1}} = [S]_{\bar{2},\hat{2}} = [S]_{\hat{2},\bar{2}} = [0]$. The proof thereby follows directly from (A.2) and (A.3).

THEOREM 6. For an odd/even excitation function $\tilde{\phi}(\tau + \hat{\tau}_0) = -\tilde{\phi}(-\tau + \hat{\tau}_0)$, $\tilde{\phi}(\tau + \bar{\tau}_0) = \tilde{\phi}(-\tau + \bar{\tau}_0)$ the determinant $\bar{\Delta}_2$ is equal to the determinant $\hat{\Delta}_2$ by a change of sign for the parameter q, i.e. $\bar{\Delta}_2(q, \ldots) = \hat{\Delta}_2(-q, \ldots)$.

Proof. When $\tilde{\phi}$ is described by $a_k \neq 0$ only for $k = 2, 6, 10, \ldots$, then as seen from (A.8), with a change of sign of q, $[S]_{\bar{2},\bar{2}}$ will only differ from $[S]_{\hat{2},\hat{2}}$ in the signs of the elements whose sum of suffices are odd. According to Muir [8] p. 25, this does not alter the determinant.

THEOREM 7. When the excitation function originates from a Fourier expansion of $(1 + b\cos\tau)^{-1}$ where $|b| < 1$, we have $a = q$ and $a_{2p} = a_2^p$ for $p = 2, 3, \ldots$, with all other $a_k = 0$. For this case with no damping ($c = 0$) we have $\bar{\Delta}_1 = 2q\hat{\Delta}_1$ and thereby no instability domains corresponding to π-period solutions.

Proof. The excitation function is treated in [3], but without the proof to be given here. Inserting $a = q$ and $a_{2p} = a_2^p$ in (A.4) we get

$$[S]_{\bar{1},\bar{1}} = \left[\begin{array}{l} 2q\,,\, 2a_2q\,,\, 2a_2^2q\,,\, 2a_2^3q\,, \\ \quad a_2^2q + q - 4\,,\, a_2(1 + a_2^2)q\,,\, a_2^2(1 + a_2^2)q\,, \\ \qquad\qquad a_2^4q + q - 16\,,\, a_2(1 + a_2^4)q\,, \\ \text{symmetric} \end{array}\right.$$

By row operations the determinant of this matrix is

$$\bar{\Delta}_1 = \left|\begin{array}{l} 2q\,,\, 2a_2q\,,\, 2a_2^2q\,,\, 2a_2^3q\,, \\ 0\,,\, -a_2^2q + q - 4\,,\, a_2(1 - a_2^2)q\,,\, a_2^2(1 - a_2^2)q\,, \\ 0\,,\, a_2(1 - a_2^2)q\,,\, -a_2^4q + q - 16\,,\, a_2(1 - a_2^4)q\,, \\ \end{array}\right.$$

which is seen to be directly proportional to the determinant of $[S]_{\hat{1},\hat{1}}$ as given by (A.5) when $a = q$ and $a_{2p} = a_2^p$ is inserted.

REFERENCES

[1] P. Pedersen, *Stability of the solutions to Mathieu-Hill equations with damping*, Ingenieur-Archiv, Vol. 49, 1980, pp. 15–29

[2] A. H. Nayfeh and D. T. Mook, *Nonlinear oscillations*, John Wiley & Sons, New York 1979, p. 704

[3] P. Pedersen, *A quantitative stability analysis of the solutions to the Carson-Cambi equation*, J. Franklin Institute, **39**, 359–367 (1980)

[4] R. Tobey *et al.*: PL/1 FORMAC *symbolic mathematics interpreter*, IBM, 360D-03.3.004, 1969, p. 164

[5] Jarl Jensen, *Tensor formac, interaktivt formac* (in Danish), Solid Mechanics, Technical Univ. of Denmark, 1978

[6] SYSTEM/360 *Continuous System Modeling Program*, IBM, GH20-0367-4, 1972

[7] F. R. Gantmacher, *The theory of matrices*, Vol. 1, Chelsea Publ. Co., New York, 1977, p. 374

[8] T. Muir, *A treatise on the theory of determinants*, Dover, 1960, p. 766